 doi:10.20944/preprints202103.0386.v1

Effect of doping $Cd_{1-x}Zn_xS/ZnS$ core/shell quantum dot in negative dielectric anisotropy nematic liquid crystal *p*-methoxybenzylidene p-decylaniline

Ayushi Rastogi[1*], Fanindra Pandey[2*], Rajiv Manohar[1*], Shri Singh[2*]

[1] Department of Physics, University of Lucknow, UP- 226007, India;

rastogiayu19@gmail.com;rajiv.manohar@gmail.com

[2] Department of Physics, Banaras Hindu University, Varanasi, UP - 221005, India;

Fanindrapatipandey143@gmail.com; srisingh@bhu.ac.in

Correspondence: Ayushi, Fanindra, Rajiv, Shri

Abstract

We report the effect of doping $Cd_{1-x}Zn_xS/ZnS$ core/shell quantum dot (CSQDs) in nematic liquid crystal *p*-methoxybenzylidene p-decylaniline (MBDA) at 0.05 wt/wt%, 0.1 wt/wt%, 0.15 wt/wt%, 0.2 wt/wt%, 0.25 wt/wt% and 0.3 wt/wt% concentrations of CSQDs in MBDA. Dielectric parameters with and without bias with respect to frequency has been investigated. The change in electro - optical parameters with temperature has also been demonstrated. The increase in the mean dielectric permittivity has been found due to large dipole moment of CSQDs which impose stronger interactions with the liquid crystal molecules. The dielectric anisotropy changes sign on doping CSQDs in MBDA liquid crystal. It was concluded that the CSQDs doping noticeably increases the dielectric permittivity of nematic MBDA in the presence of electric field. The doping of CSQDs in nematic MBDA liquid crystal reduces the ion screening effect effectively. This phenomenon is attributed to the competition between the generated ionic impurities during assembling process and the ion trapping effect of the CSQDs. The rotational viscosity of nematic liquid crystal decreases with increasing concentration of the CSQDs with faster response time observed for 0.05 wt/wt% concentration. The birefringence of the doped system increases with the inclusion of CSQDs in MBDA. These results find application in the field of display devices, phase shifters, industries and projectors.

Keywords: Nematic liquid crystal MBDA; core/shell QDs (CSQDs); Dielectric, electro optical parameters; photonic displays

Preprints (www.preprints.org) | NOT PEER-REVIEWED | Posted: 15 March 2021 doi:10.20944/preprints202103.0386.v1

1. Introduction

Negative dielectric anisotropy ($\Delta\varepsilon < 0$) liquid crystals have been extensively employed in direct-view and projection displays [1]. The widespread feature of a negative $\Delta\varepsilon$ liquid crystal is that lateral polar substituents induce a dipole moment perpendicular to the principal molecular axis [2, 3]. As explained in the reference [4], there are quite a lot of techniques to induce polarity perpendicular to the molecular axis, such as (i) using certain polar linking groups; (ii) A cyclohexane ring involving a polar unit at an axial position; (iii) An aromatic ring with polar unit(s) in lateral positions; and (iv) use of heterocyclic rings with the heteroatom off-axis. However, the aspect ratio of the cylindrical molecular shape would decrease by the off-axis polar group which tends to disturb the liquid crystal phase stability [4]. An adequately large $\Delta\varepsilon$ facilitates lower driving voltage, which in turn lowers the power consumption of display devices. Most nematic liquid crystal devices involve surface alignment layers in order to comprehend their electro - optic effect. A negative $\Delta\varepsilon$ liquid crystal can be utilized in planar or vertical alignment, depending on the electric field direction or mixing suitable dopant. In an in-plane switching (IPS) cell [5] or fringe-field switching (FFS) cell [6], the electric field is mainly in the lateral direction, while in a vertically aligned cell [7] or multi-domain vertical alignment cell [8], the field is directed in the longitudinal direction. For mobile displays, IPS or FFS is a favored choice because they are more robust to external pressure, which is crucial for touch panels [9]. In this paper, we will focus on the negative dielectric anisotropy ($\Delta\varepsilon$) nematic liquid crystal doped with $Cd_{1-x}Zn_xS/ZnS$ core/shell quantum dots (CSQDs) for its applications in display devices, phase shifters, antennas.

Basu et al. [10] provided the evidence for the formation of self assembly of CdS QDs in 5CB nematic liquid crystal. Gupta et al. [11], illustrated the phase retardation behavior of nematic 8CB (positive $\Delta\varepsilon$) doped with CdSe QDs. It explained the formation of self assembled arrays of QDs in nematic liquid crystal and thus, the improved alignment in doped systems was observed. Seidalilir et al. [12], reported the improved electro chemical and electro – optical properties of Ni:ZnCdS/ZnS core/shell QDs in positive $\Delta\varepsilon$ nematic E7 liquid crystal. It explained the self assembled arrays of CSQDs in nematic phase and reduction in the screening effect by ion trapping effect of CSQDs. Misra et al. [13], explained the influence of dispersing Cu:ZnO in

Preprints (www.preprints.org) | NOT PEER-REVIEWED | Posted: 15 March 2021 doi:10.20944/preprints202103.0386.v1

nematic MBBA liquid crystal and studied the dielectric properties and activation energies for the dispersed systems. Singh et al. [14], reviewed the effect of doping nanoparticles in nematic liquid crystals. Rastogi et al. [15], reported the effect of doping graphene oxide (GO) in negative Δε nematic *p*-methoxybenzylidene p-decylaniline (MBDA) liquid crystal and found that the rotational viscosity, threshold voltage increases with increase in concentration of GO in MBDA. GO effectively traps the ionic impurities in doped systems which results in improved dielectric properties. The schematic illustration of ion capturing phenomenon of $Cd_{1-x}Zn_xS/ZnS$ CSQDs in nematic 2020 has been demonstrated by Rastogi et al. [16]. Pandey et al. [17], investigated the dielectric and electro – optical properties of felix 17/000 ferroelectric liquid crystal doped with $Cd_{1-x}Zn_xS/ZnS$ core/shell quantum dot. The lower operating voltage with faster optical response time was noticed. Singh et al. [18], reported the quenching in photoluminescence intensity with improved contrast of felix 17/000 by doping $Cd_{1-x}Zn_xS/ZnS$ CSQDs. The impact of doping CSQDs in negative Δε nematic liquid crystal BBHA on its dielectric and electro – optical properties has been examined by Tripathi et al. [19]. It was found that the relaxation frequency of doped system was shifted to higher frequency side with bias voltage with improved birefringence and response time. The doping of $Cd_{1-x}Zn_xS/ZnS$ CSQDs in negative Δε (-1.36) nematic liquid crystal MBDA has never been reported so far. Therefore, the present paper deals with the doping of $Cd_{1-x}Zn_xS/ZnS$ core/shell quantum dot (CSQDs) in nematic liquid crystal MBDA. The dielectric and electro - optical measurement has been performed for different concentration of CSQDs abbreviated as Mix 1, Mix 2, Mix 3, Mix 4, Mix 5 and Mix 6. The dynamic behavior of a mixture consisting of liquid crystalline MBDA and CSQDs in electric field has been studied. The model is based on elastic continuum theory considering the interaction of the nematic molecules with the surrounding molecules [20]. The main findings of the work reveals faster electro – optic response time, reduced rotational viscosity and improved birefringence for Mix 1. The self assembled arrays of CSQDs in MBDA liquid crystal improves the orientational order and alignment of doped systems. The dielectric anisotropy reveals the change in the sign of Δε for doped system as compared to pure nematic MBDA. CSQDs effectively trap the ionic charges on its surface thus ablating the screening effect, leading to improved dielectric and electro – optical properties.

2. Experimental Details

Preprints (www.preprints.org) | NOT PEER-REVIEWED | Posted: 15 March 2021 doi:10.20944/preprints202103.0386.v1

The nematic liquid crystal material used in this study is negative dielectric anisotropy *p*-methoxybenzylidene *p*-decylaniline (MBDA) which exhibits the following chemical structure and phase sequence as shown in Figure. 1 [15]. MBDA has been obtained from Frinton Laboratories Inc. USA. The optical anisotropy of MBDA is as follows: Δn_{MBDA}= 0.05 (56°C, at 693.2 nm wavelength). We have used negative dielectric anisotropic liquid crystal $\Delta\varepsilon$= -1.36.

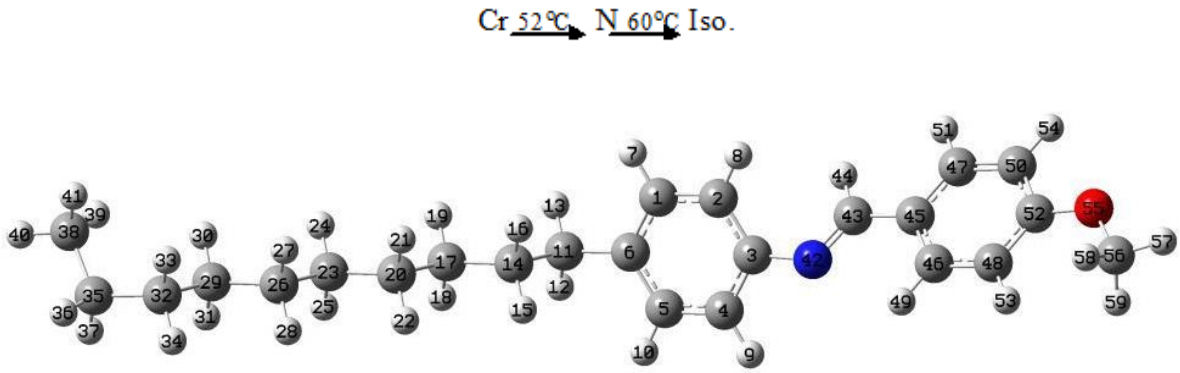

Figure.1 Optimized chemical structure of *p*-methoxybenzylidene p-decylaniline (MBDA).

CSQDs have been doped in MBDA liquid crystal. It has been synthesized by Gram-scale one pot synthesis method as described by Bae et al. [21]. The TEM and XRD characterization of CSQDs has already been provided in [18]. $Cd_{1-X}Zn_XS/ZnS$ (x= 0.85) core/shell implemented in the present study has the diameter of about 8.5 nm. x = 0.85 yields high luminescence of blue emission and photoluminescence quantum yield. The core (diameter 5 nm) has been well protected by the layer surrounding it called shell (diameter 3.5 nm). ZnS shell act as a capping agent. The role of ZnS shell over the $Cd_{1-X}Zn_XS$ core has been reported by D. Bera et al. [22].

The fabrication of sample cell holder has been done by the method as described in our work [15]. It involves the use of conducting indium tin oxide (ITO) glass plates. Photolithographic technique was used to achieve desired electrode pattern on the ITO substrates [15]. The active electrode area was 5×5mm^2. In order to achieve planar alignment rubbed polyimide technique was being used. In this technique, the planar alignment has been achieved by treating the conducting layer with adhesion promoter and polymer nylon (6/6). After drying the polymer layer, substrates were rubbed unidirectional in antiparallel manner. The capacitor is formed by placing the substrates one over another. The thickness of the sample cells used in the present study is 8 μm. The empty sample cells were calibrated using analytical reagent (AR)

Preprints (www.preprints.org) | NOT PEER-REVIEWED | Posted: 15 March 2021 doi:10.20944/preprints202103.0386.v1

Benzene (C_6H_6). CSQDs and MBDA nematic liquid crystal composites were prepared by incorporating the desired concentration of CSQDs with pure MBDA. For that, wt/wt ratio of CSQD was dispersed into the pure MBDA and then homogenized with an ultrasonic mixer for uniform mixing of CSQDs. The CSQDs doped MBDA composites are named as Mix 1 (0.05 wt/wt %), Mix 2 (0.1 wt/wt%), Mix 3 (0.15 wt/wt%), Mix 4 (0.2 wt/wt%), Mix 5 (0.25 wt/wt%) and Mix 6 (0.3 wt/wt%). Pure MBDA and CSQDs doped nematic liquid crystal materials were filled inside the cells in isotropic phase by means of capillary action and then slowly cooled down to room temperature.

2.1 Preparation of homogenous mixture of CSQDs and MBDA composites

A suspension of CSQDs (1 mg/ml) was prepared in toluene and ultrasonicated for 2 h to ensure the homogenous suspension. Fixed amount of MBDA nematic liquid crystal was doped with different weight percentage concentration of CSQDs by taking 0.05 wt/wt%, 0.1 wt/wt %, 0.15 wt/wt%, 0.2 wt/wt%, 0.25 wt/wt% and 0.3 wt/wt% concentration of CSQDs in MBDA. CSQDs and MBDA composites were then homogenized by magnetic stirring for 4 h at an isotropic temperature followed by ultrasonication for next 3 h. This procedure was repeated several times to obtain the homogenous mixture of CSQDs in MBDA. Toluene was evaporated at an elevated temperature with slow evaporation rate. The liquid crystal sample cells were filled by capillary method.

The dielectric measurements has been performed using computer-controlled HP 4194A impedance gain/phase analyzer using Temperature controller (mK 2000, Instec Co. USA) interfaced with computer software Wintemp used to maintain the temperature of the hot plate (Instec HCS-302) with an accuracy of ± 0.001 °C.

For electro optical set up: He–Ne laser (5 mW power, 693.2 nm wavelength), Programmable function generator (Tektronix, AFG-3021B), Photodetector (Instec PD02-L1), Digital storage oscilloscope (Tektronix, TDS-2024C, Temperature controller (mK 2000, Instec Co. USA) interfaced with computer software Wintemp used to maintain the temperature of the hot plate (Instec HCS-302) with an accuracy of ± 0.001 °C has been used.

3. Result and Discussion

3.1 Polarizing Optical Micrographs

Preprints (www.preprints.org) | NOT PEER-REVIEWED | Posted: 15 March 2021 doi:10.20944/preprints202103.0386.v1

The polarizing optical micrographs for pure MBDA and its doped system with CSQDs (Mix 1 to Mix 6) at 56° C temperature have been shown in Figure 2 under crossed polarizer condition. The uniform molecular alignment is clearly depicted from these texture images. Mix 1 shows maximum light transmission with improved alignment and hence exhibits increased brightness in comparison to other mixtures and pure MBDA liquid crystal. This result is also evident from birefringence measurement discussed in the later part of this paper.

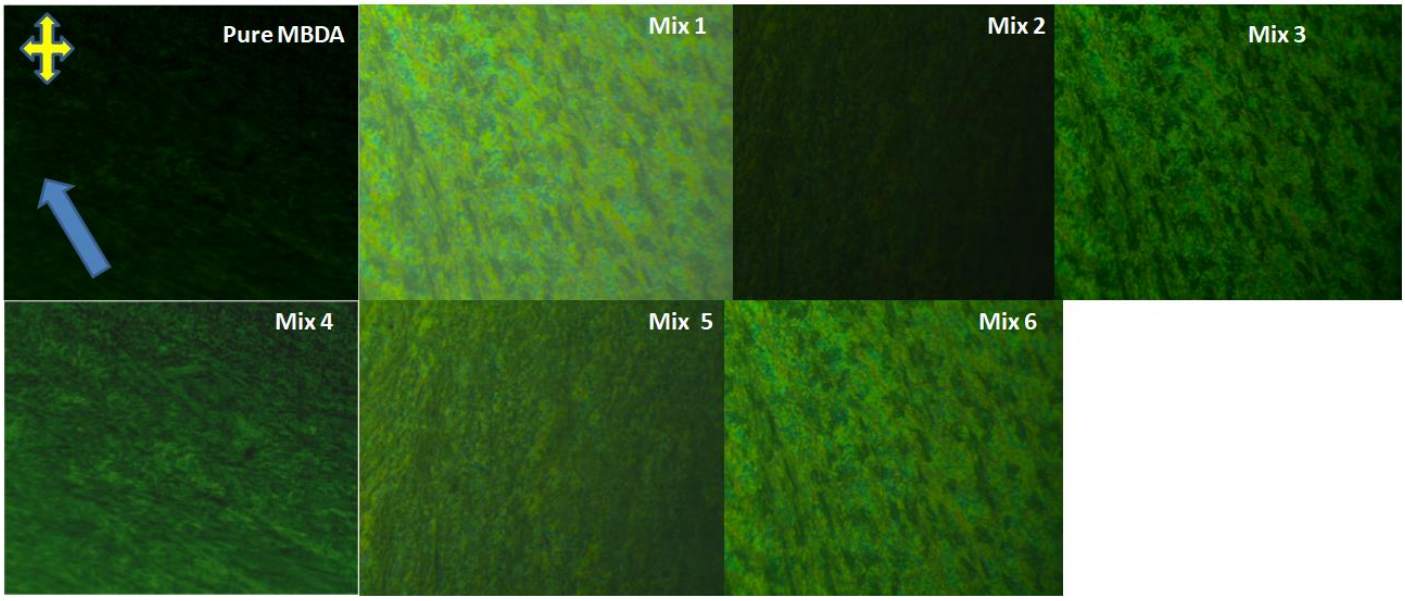

Figure.2 Polarizing optical micrographs for pure nematic MBDA and its mixture with core/shell quantum dot (Mix 1 to Mix 6) at 56° C temperature.

3.2 Dielectric Response and Dielectric Anisotropy

In an aligned nematic phase the ac electric field produces the transverse molecular rotation i.e., the molecular rotation about short axis in low frequency range and longitudinal molecular rotation i.e., about long axis at high frequencies [13]. However, in the experimental window of the frequency, the relaxation mode about the long axis of the molecular rotation cannot be detected and the relaxation mode about its short axis is usually observed. In the existence of relaxation phenomenon, the dielectric constant can be explained as a complex quantity,

$$\varepsilon^*(\omega) = \varepsilon'(\omega) - j\varepsilon''(\omega) \quad \text{---------- (1)}$$

Preprints (www.preprints.org) | NOT PEER-REVIEWED | Posted: 15 March 2021 doi:10.20944/preprints202103.0386.v1

Here, $\varepsilon'(\omega)$ and $\varepsilon''(\omega)$ represents the real and imaginary parts of the complex dielectric constant function $\varepsilon^*(\omega)$. On separating the real and imaginary parts of equation (3) and adding the high and low frequency correction terms, we get [23],

$$\varepsilon' = \varepsilon'(dc)f^{-n} + \varepsilon'(\infty) + \frac{\delta\varepsilon'[1+(2\pi f\tau)^{(1-\alpha)}\sin(\alpha\pi/2)]}{1+(2\pi f\tau)^{2(1-\alpha)}+2(2\pi f\tau)^{(1-\alpha)}\sin(\alpha\pi/2)} \quad \text{---------(2)}$$

$$\varepsilon'' = \frac{\sigma(dc)}{\varepsilon_0 2\pi f^{k}} + \frac{\delta\varepsilon'(2\pi f\tau)^{(1-\alpha)}\cos(\alpha\pi/2)}{1+(2\pi f\tau)^{2(1-\alpha_{GM})}+2(2\pi f\tau)^{(1-\alpha)}\sin(\alpha\pi/2))} + Af^{m} \quad \text{----------(3)}$$

Here σ (dc) is ionic conductance and ε_o is free space permittivity, k is fitting parameter and ω is angular frequency. The term ε (dc)/f^{-n} and σ(dc)/ $\varepsilon_o 2\pi f^k$ are added in above equation for low frequency effect due to the electrode polarization, capacitance and ionic conductance. The term Af^m term is added in equation for high frequency effect due to the ITO resistance and lead inductance. By the least square fitting of above equation into experimental data we have removed the low and high frequency errors.

3.2.1 Dielectric Response at Planar Geometry

The variations of the perpendicular components of dielectric permittivity ($\varepsilon'_\perp$) and dielectric loss ($\varepsilon''_\perp$) of pure MBDA and CSQDs doped system (Mix 1 to Mix 6) with frequency at a temperature 56° C for the planar orientation has been shown in Figure 3 (a, b).

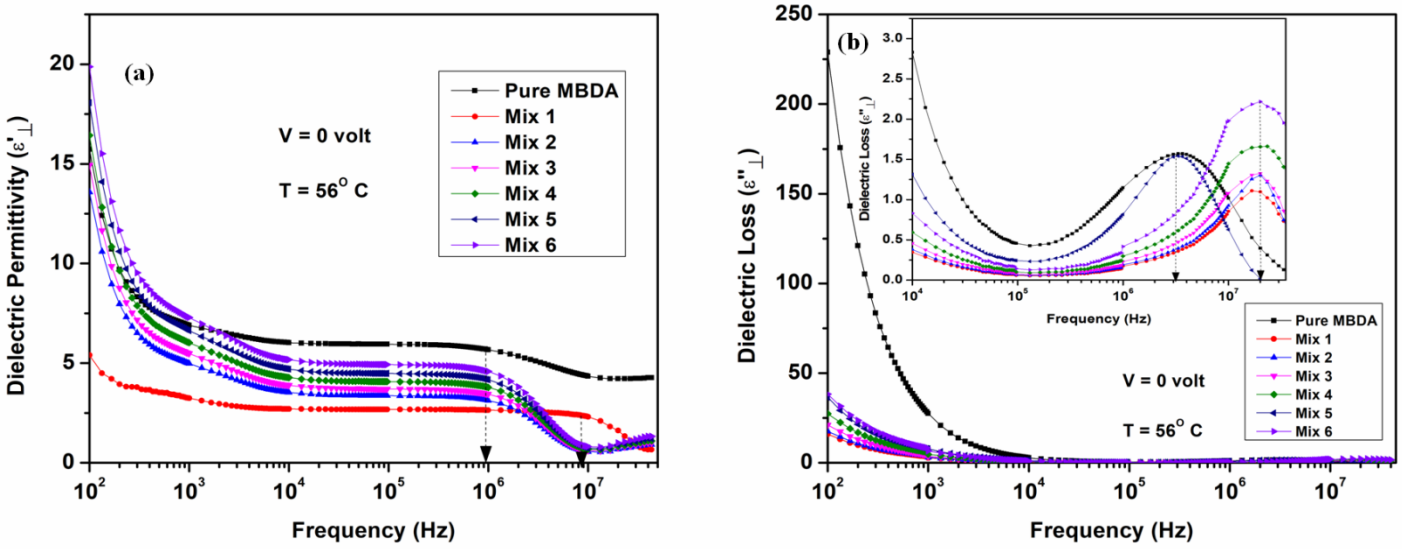

Preprints (www.preprints.org) | NOT PEER-REVIEWED | Posted: 15 March 2021 doi:10.20944/preprints202103.0386.v1

Figure.3 (a) Variation of dielectric permittivity versus frequency at 0 volt applied bias and 56^{o}C temperature for pure nematic MBDA and its mixture with core/shell quantum dot (Mix 1 to Mix 6); **(b)** Variation of dielectric loss versus frequency at 0 volt applied bias and 56^{o}C temperature for pure nematic MBDA and its mixture with core/shell quantum dot (Mix 1 to Mix 6).

It can be seen from Figure 3 (a, b) that for the planar orientation both the perpendicular component of dielectric permittivity and dielectric loss depends strongly on the concentration of CSQDs in host nematic MBDA. Decrement in the magnitude of $\varepsilon'_{\perp}$ is observed with the increase in the concentration of CSQDs. In the frequency range 1 kHz to 900 kHz the $\varepsilon'_{\perp}$ remains almost constant for pure MBDA whereas for Mix 1 to Mix 6, $\varepsilon'_{\perp}$ remains constant for frequency range 1 kHz to 9 MHz however, at higher frequencies rapid decrease in its values are observed. This can be explained on the basis of dipolar interaction [13, 16] between the CSQDs and nematic MBDA molecules. It is well known that in the absence of electric field the dipole moments of CSQDs and nematic molecules do not align parallel to each other. The dielectric properties depend on the anchoring energy, orientations, shape and size of CSQD molecules. The dielectric relaxation spectra in pure and CSQD doped system correspond to the rotation about the short molecular axes. The relaxation frequency mainly depends on the anchoring energy and orientational order parameter. It can be observed from Figure 3 (b) that the dielectric loss are higher in low frequency region (< 10 MHz) for both the pure MBDA and CSQD doped system and with increasing frequency the values decrease, remaining constant in the frequency regime 10 kHz to 100 kHz and then start increasing with maxima at relaxation frequencies. The low-frequency regime reveals the induced polarization due to Maxwell – wagner space charge polarization effect by the electrode and interface polarizations and above 10 MHz is dominated by the ITO sheet resistance effect [23]. The maxima of the dielectric loss spectrum in the frequency range greater than 100 kHz show the dielectric relaxation polarization of the short axis in the nematic molecules. The relaxation phenomenon is attributed to the interaction of CSQDs and nematic MBDA molecules and it can be due to the contribution of orientations of the nematic molecules. The relaxation frequency of pure MBDA has been observed at 900 kHz and for the doped systems (Mix 1 to Mix 6) at 9 MHz. The relaxation frequency shifts towards higher side with increasing the concentration of CSQDs in pure MBDA. It has been stated that the relaxation process of pure and CSQDs doped system (Mix 1 to Mix 6) is dominated by molecules located,

Preprints (www.preprints.org) | NOT PEER-REVIEWED | Posted: 15 March 2021 doi:10.20944/preprints202103.0386.v1

at the surface and in bulk regions, respectively [13]. Relaxation frequency is lower in the surface layer, because the surface viscosity is greater than the bulk viscosity in pure nematic.

3.2.2 Dielectric Response at Homeotropic Geometry

The variations of dielectric permittivity $\varepsilon'_{\parallel}$ and dielectric loss ($\varepsilon''_{\parallel}$) with frequency for homeotropic orientation at 56° C has been shown in Figure 4 (a, b).

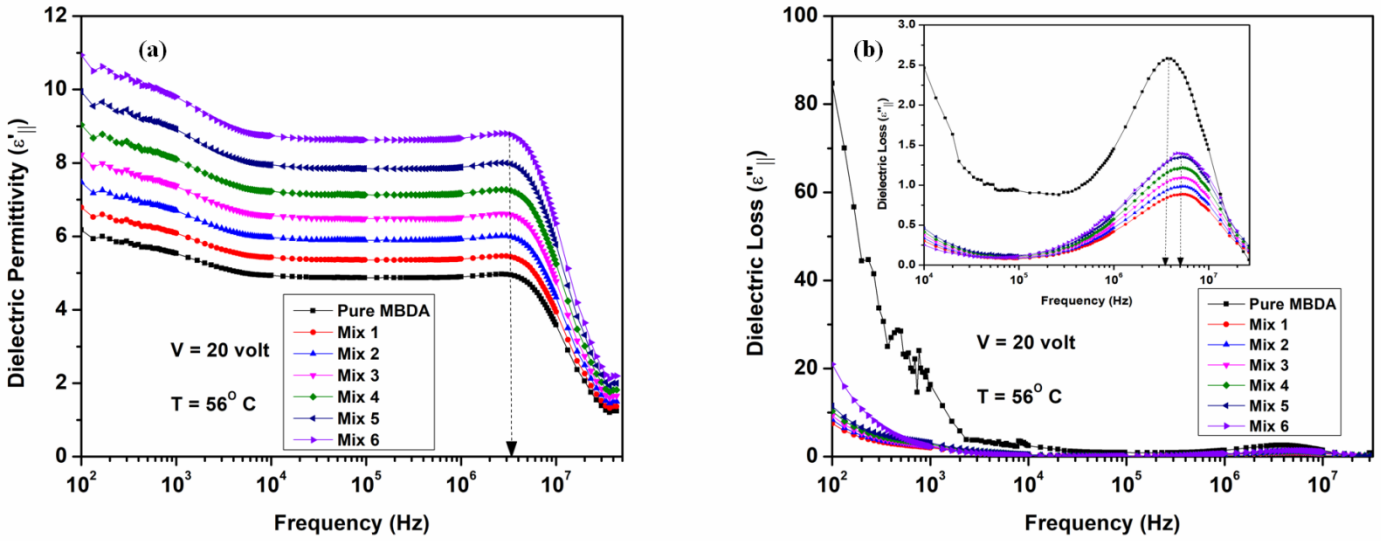

Figure.4 (a) Variation of dielectric permittivity versus frequency at 20 volt applied bias and 56°C temperature for pure nematic MBDA and its mixture with core/shell quantum dot (Mix 1 to Mix 6); **(b)** Variation of dielectric loss versus frequency at 20 volt applied bias and 56°C temperature for pure nematic MBDA and its mixture with core/shell quantum dot (Mix 1 to Mix 6).

It has been observed that $\varepsilon'_{\parallel}$ increases with the concentration of CSQDs in nematic MBDA contrary to planar orientation discussed earlier. However, trend remains same in geometries, the $\varepsilon'_{\parallel}$ remains almost constant from 1MHz to 3.5 MHz and then decrease rapidly. The dielectric relaxation frequency of pure MBDA and CSQDs doped system (Mix 1 to Mix 6) has been found at 3.5 MHz. In the presence of electric field when CSQDs are doped with nematic MBDA, the dipole moments of nematic molecules gets align with the dipole moments of CSQDs molecules because of the generation of the local electric field. This might be the reason for the increase in the value of $\varepsilon'_{\parallel}$ for the doped systems (Mix 1 to Mix 6). Hence, in CSQDs doped system there is formation of numerous domains in the bulk region. There exists three

Preprints (www.preprints.org) | NOT PEER-REVIEWED | Posted: 15 March 2021 doi:10.20944/preprints202103.0386.v1

kinds of interactions namely, CSQDs - CSQDs, CSQDs - nematic and nematic - nematic in the doped systems [16]. The decrease in relaxation frequency with bias voltage has been attributed to the weak anchoring strength in the homeotropic orientation, occurring due to the reorientations of nematic molecules. Notably, CSQDs molecules share their intrinsic properties with the host MBDA due to the alignment with MBDA molecules. The fluctuations in the orientational order parameter increase the rotational viscosity which may be responsible for the increase in the relaxation frequency without bias voltage. Although the dipole moment of MBDA molecules and CSQDs get align along the direction of electric field but at the surface, nematic molecules do not get align in the same direction due to anchoring energy. Furthermore, at low concentration of CSQDs (Mix 1) interaction between MBDA molecules plays considerable role but at higher concentration of CSQDs, the CSQDs – CSQDs interaction govern the role so the magnitude of $\varepsilon'_{\parallel}$ increases with the concentration of CSQDs in nematic MBDA.

3.2.3 Dielectric anisotropy and Mean Dielectric Constant

The non uniform distribution of charges in the mesogenic molecules induces the electric dipole moment in liquid crystals which makes an angle with the long axis of the mesogens. The overall dipole moment is then resolved into two dielectric components; one along the long axis of the mesogen $\varepsilon'_{\parallel}$ and another perpendicular to it i.e.,$\varepsilon'_{\perp}$ [23]. The anisotropic polarizability and the geometrical shape of the liquid crystal molecules increases the Vander Waals energy, and thus the axes with the largest polarizability will be aligned parallel to each other [13]. The dielectric components ($\varepsilon'_{\parallel}$ and $\varepsilon'_{\perp}$) difference yields the dielectric anisotropy (Δε).

The sign of Δε can be either a positive or negative accordingly as whichever dielectric component is greater. The director reorientation in the presence of electric field is generally associated with the value of Δε. In nematic liquid crystals, the dielectric response is determined by the molecular rotation about its short axis or long axis [16]. The measured dielectric permittivities of pure nematic MBDA and its mixture with CSQDs with the two orientations and their corresponding Δε ($\Delta\varepsilon = \varepsilon'_{\parallel} - \varepsilon'_{\perp}$) has been found to be -1.36, 2.85, 1.72, 1.89, 2.08, 2.28 and 2.51 for pure MBDA and Mix 1 to Mix 6, at 56^{o} C temperature (Figure 5).

Preprints (www.preprints.org) | NOT PEER-REVIEWED | Posted: 15 March 2021 doi:10.20944/preprints202103.0386.v1

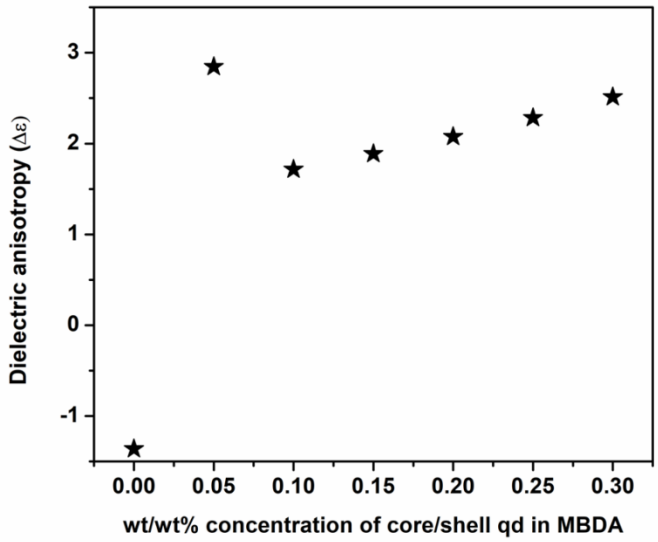

Figure.5 Dielectric anisotropy of pure nematic MBDA and its mixture with core/shell quantum dot (Mix 1 to Mix 6) at 1 kHz frequency.

The increment in the magnitude of Δε has been observed for the doped system as compared to pure MBDA system. The decrement in Δε has been attributed to the existence of strong dipolar interaction between MBDA molecules and CSQDs and reorientation MBDA molecules. The dielectric phenomenon as well as ions present in pure nematic MBDA system contributes effectively in changing the value of Δε. Both these dielectric components are temperature dependent. However, there is another parameter average dielectric permittivity $\bar{\varepsilon}$ that is known to be temperature independent [13]. The average dielectric permittivity ($\bar{\varepsilon}$) of pure MBDA and its mixture with CSQDs has been calculated by using the following equation [13]:

$$\bar{\varepsilon} = \frac{1}{3}(\varepsilon_{\parallel} + 2\varepsilon_{\perp}) \text{ ----------(4)}$$

The variation of $\bar{\varepsilon}$ at a certain temperature (56^{o} C) for the pure MBDA and its doped system with CSQDs has been shown in Figure 6.

Preprints (www.preprints.org) | NOT PEER-REVIEWED | Posted: 15 March 2021 doi:10.20944/preprints202103.0386.v1

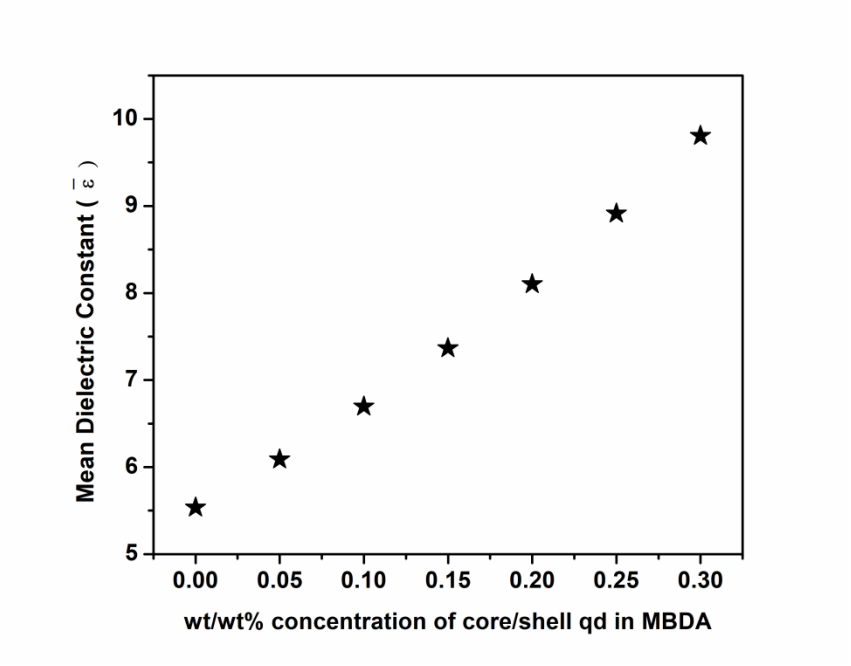

Figure.6 Mean dielectric constant of pure nematic MBDA and its mixture with core/shell quantum dot (Mix 1 to Mix 6) at 1 kHz frequency.

It has been observed that the average dielectric permittivity $\bar{\varepsilon}$ of pure MBDA increases with the addition of CSQDs. The systematic and consistent improvement in Δε and $\bar{\varepsilon}$ has been noticed for the doped system (Figure 5 & 6). This clearly illustrates that the doping of CSQDs in pure nematic MBDA increases the orientational order of the nematic molecules. This increment has been related to the polarization coupling between pure MBDA and CSQD molecules in the presence of electric field. The CSQD dipoles get aligned in the electric field direction and because of the polarization effect, the nematic molecules also gets aligned with the CSQD dipoles. This results in improvement in the orientational order parameter of the nematic molecules and thus increases the dielectric permittivity $\varepsilon'_{\parallel}$.

3.3 Electro – optical Parameters

Temperature dependent on time, off time, total electro – optic response time and rotational viscosity at 1kHz frequency, 20 volt bias has been shown in Figure 7 (a – d).

Preprints (www.preprints.org) | NOT PEER-REVIEWED | Posted: 15 March 2021 doi:10.20944/preprints202103.0386.v1

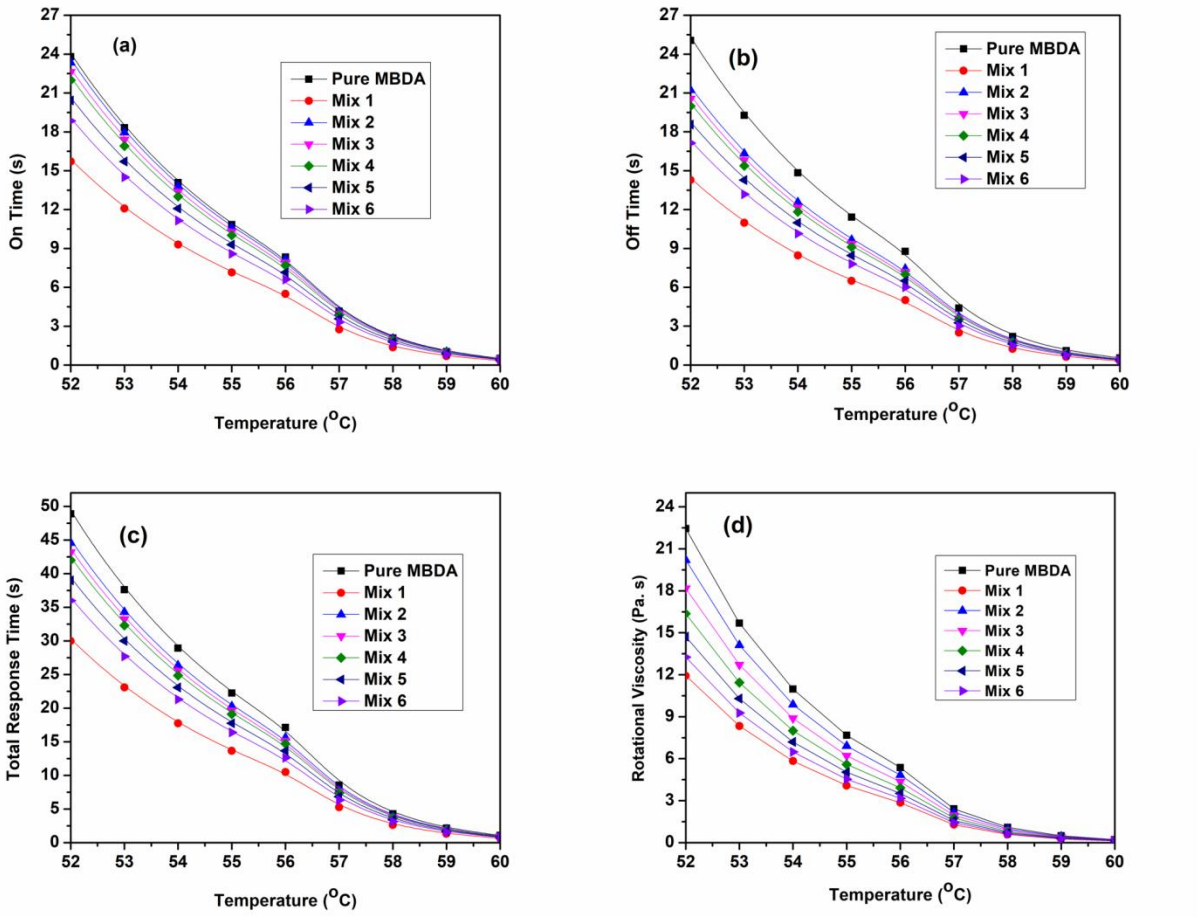

Figure.7 (a) Temperature dependent on time for pure nematic MBDA and its mixtures with core/shell quantum dot (Mix 1 to Mix 6) at 20 volt applied bias, 1 kHz frequency input signal; **(b)** Temperature dependent off time for pure nematic MBDA and its mixtures with core/shell quantum dot (Mix 1 to Mix 6) at 20 volt applied bias, 1 kHz frequency input signal; **(c)** Temperature dependent total electro – optic response time for pure nematic MBDA and its mixtures with core/shell quantum dot (Mix 1 to Mix 6) at 20 volt applied bias, 1 kHz frequency input signal; **(d)** Temperature dependent rotational viscosity for pure nematic MBDA and its mixtures with core/shell quantum dot (Mix 1 to Mix 6) at 20 volt applied bias, 1 kHz frequency input signal.

It has been observed that these electro – optical parameters decreases with increase in temperature due to increase in the kinetic energy of the system with rise in temperature. Figure 7 (a – d) shows that on time, off time, total response time and rotational viscosity follows the similar trend with fastest response time observed for Mix 1. The increase in the concentration of

Preprints (www.preprints.org) | NOT PEER-REVIEWED | Posted: 15 March 2021 doi:10.20944/preprints202103.0386.v1

CSQDs in MBDA (Mix 2 to Mix 6) results in decrease in the response time in comparison to pure MBDA (Figure 7 (a – c)). This has been attributed to reduce rotational viscosity observed for these mixtures with increasing concentration as shown in Figure 7 (d).

Both on and off times as shown in Figure 7 (a, b) and total electro – optic response time τ_{total} (Figure 7 (c)), decreases with increase in the concentration of CSQDs with fastest response observed for Mix 1. It is expected that the reason for this behavior is associated with the increase in $\Delta\varepsilon$ and the suppression of screening effect. The accumulation of ionic charges on the substrate surfaces creates an induced electric field which reduces the effective field exerted on the liquid crystal layers. Therefore, the response time of pure MBDA liquid crystal required for the display increases due to the screening effect [12, 16]. In CSQD doped MBDA samples, the CSQDs can trap ionic impurities which results in fewer ions adsorbed on the substrate surfaces and thus abating the screening effect. The 0.05 wt% (Mix 1) of CSQDs was found to be optimized dopant concentration in nematic medium from an application point of view. As discussed earlier, there are three kinds of molecular interaction governing the behavior of doped samples. Out of these interactions, Mix 1 i.e., mixture with low concentration of CSQDs possess dominating role of nematic – CSQDs interaction thus possess foster response time. On time is purely electric field driven process and is given by following relation [24]:

$$\tau_{ON} = \frac{\gamma d^2}{\varepsilon_o \Delta\varepsilon \, (V^2 - {V_{th}}^2)} \quad \text{----------(5)}$$

Here symbols have usual meaning; τ_{on} is on time, V is the applied voltage, V_{th} is threshold voltage, γ is rotational viscosity and d is the thickness of sample cell. Fall time or off time τ_{off} of the director depends on the rotational viscosity and anchoring energy (K), is given as:

$$\tau_{OFF} = \frac{\gamma d^2}{K.\pi^2} \quad \text{---------- (6)}$$

$$\tau_{total} = \tau_{on} + \tau_{off} \quad \text{---------- (7)}$$

The rotational viscosity (Figure 7 (d)) represents the internal friction among nematic molecules during their rotation motion, which is an important characteristic that affects the field-induced switching behavior of the nematics [25]. It mainly depends on the anchoring energy and off time. The combined influence of optical, magnetic and electrical properties in multifunctional CSQDs produces the significant change in pure MBDA nematic liquid crystal. Therefore, doping of multifunctional CSQDs can improve the electrical conductivity and hence decrease the rotational viscosity of pure nematic MBDA. On the other hand, the formation of self assembled

Preprints (www.preprints.org) | NOT PEER-REVIEWED | Posted: 15 March 2021 doi:10.20944/preprints202103.0386.v1

chain of CSQDs along the mesogenic director in nematic liquid crystal cell and their agglomeration in nematic phase provides new path to facilitate the charge transportation in the nematic cell. This leads to decrease rotational viscosity in the nematic medium. A noteworthy point that should be concerned is the existence of ionic impurities in the nematic medium that can limit the charge transportation and therefore increase the rotational viscosity of nematic medium. The incorporation of CSQDs in nematic medium results in the adsorption of ionic impurities by the CSQDs, which causes reduction in the ionic density and the resistance of the nematic medium. Consequently, the rotational viscosity of CSQDs doped MBDA system gets reduced with faster response observed for doped system. In the presence of applied bias, induced dipole moments of the CSQDs can proficiently trap the ionic impurities in the nematic host, leading to a decrease in the rotational viscosity. On the other hand, the CSQDs themselves act as external additives in the nematic host which can increase the rotational viscosity when the concentration of CSQDs is too low below 0.05%. The reason associated with this behavior is that the too low concentration of CSQDs cannot efficiently trap the ionic impurities present in nematic medium therefore the ionic impact dominates over its reduction.

Temperature dependent birefringence for pure MBDA and its doped system with CSQDs (Mix 1 to Mix 6) at 20 volt, 1 kHz frequency input signal has been shown in Figure 8.

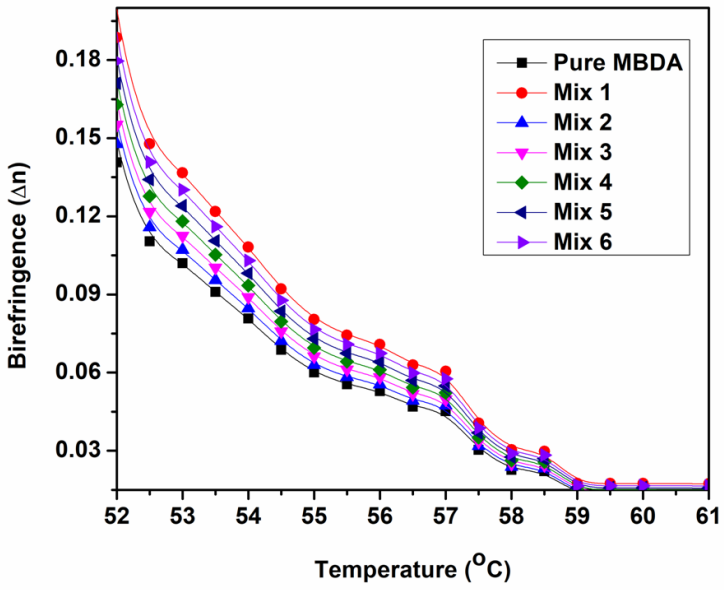

Figure.8 Variation of birefringence with temperature for pure nematic MBDA and its mixture with core/shell quantum dot (Mix 1 to Mix 6).

Preprints (www.preprints.org) | NOT PEER-REVIEWED | Posted: 15 March 2021 doi:10.20944/preprints202103.0386.v1

In the present work, the birefringence has been calculated from the given relation [24]:

$$\Delta n = \left[\frac{\lambda}{2\times\pi\times d}\right]\times\Delta\phi \text{ ----------(8)}$$

$$\Delta\phi = m\pi + 2\sin^{-1}\sqrt{\frac{I - I_{min}}{I_{max} - I_{min}}} \text{ ----------(9)}$$

m = 0, 2, 4…….

$$\Delta\phi = (m+1)\pi - 2\sin^{-1}\sqrt{\frac{I - I_{min}}{I_{max} - I_{min}}} \text{ ----------(10)}$$

m= 1, 3, 5, 7……

Here, m is the maximum number of peaks observed in intensity versus temperature graph. I is the voltage dependent intensity values, I_{max} and I_{min} are the maximum and minimum intensities, λ is wavelength and phase retardation (ΔΦ)

It has been observed that the birefringence increases with increase in concentration of CSQDs in MBDA and Mix 1 exhibits maximum birefringence. The improved molecular alignment and orientational order is responsible for maximum birefringence observed in Mix 1 which is evident from texture and dielectric studies discussed earlier. The increase in Δε with increase in concentration of CSQDs improves the molecular ordering in the doped systems which consequently produces the phase difference between extraordinary and ordinary light rays. Thus, the birefringence of the pure and doped system is given as:

$\Delta n = n_e - n_o$ ---------- (11)

Here, n_e and n_o are the refractive indices of extraordinary and ordinary rays. The schematic illustration of optical model of birefringence has been depicted by Gupta et al. [11]. For negative Δε nematic MBDA liquid crystal; $n_e < n_o$ therefore, the velocity of extraordinary ray which follows the elliptical path will be greater than the velocity of ordinary ray which follows the circular path hence in this case the circle will be formed inside the ellipse. For positive Δε systems (Mix 1 to Mix 6); $n_e > n_o$ therefore, both components of light ray follow opposite path.

Conclusion

In this work, we investigated the effects of luminescent $Cd_{1-x}Zn_xS/ZnS$ core/shell QDs on the dielectric and electro - optical properties of nematic MBDA liquid crystal. The analysis of

 doi:10.20944/preprints202103.0386.v1

dielectric spectra in the presence of bias voltage indicated that doping a nematic host with CSQDs significantly increases the dielectric permittivity of nematic liquid crystal whereas without bias voltage the dielectric permittivity decreases with the concentration of CSQDs in MBDA. The presence of CSQDs affects the molecular ordering as well as influenced the dielectric parameters significantly. These changes are attributed to the change in the overall dipole moment of pure and doped systems. The frequency dependent dielectric loss spectra indicate the shift in relaxation frequency with and without bias which is explained on the basis of effective interaction between nematic and CSQD molecules. The ionic impurity decreases with the addition of CSQDs. These effects are attributed to the ionic harvest effect of the CSQDs. The effect of CSQDs on the dielectric and electro-optical properties such as dielectric anisotropy, rotational viscosity, field- on and field-off response time was also studied. The results showed that the dielectric anisotropy increases with increasing the CSQDs concentration and found to be maximum for Mix 1 due to the formation of 1D arrays of CSQDs along the nematic director and the increased order parameter in the bulk nematic liquid crystal. Furthermore, the rotational viscosity was strictly dependent on the anchoring energy and field – off time and it decreases with the addition of CSQDs in MBDA. The enhanced birefringence of doped system has been attributed to its improved alignment. This has been attributed to an increase in dielectric anisotropy and the suppression of the screening effect.

CREdiT Authorship Contribution Statement

Ayushi Rastogi: Conceptualization, Methodology, Validation, Data curation, Resources, Writing - original draft, Writing – review & editing. **Fanindra Pati Pandey:** Conceptualization, Methodology, Validation, Data curation, Writing - original draft, review & editing. **Rajiv Manohar:** Conceptualization, Validation, Methodology, Resources, Writing - review & editing. **Shri Singh:** Conceptualization, Validation, Methodology, Resources, Writing - review & editing.

Disclosure Statement

All authors report no conflict of interest.

Acknowledgement

Ayushi Rastogi is thankful to UGC (F-25-1/2014-15(BSR)/ 7-177/2007/BSR) New Delhi for UGC-BSR Fellowship. Author Rajiv Manohar acknowledges UGC for the grant of a MID Career Award dated 22 March 2018 [No.F.19-224/2018 (BSR)]. Authors are thankful to Centre

of Excellence at APJ Abdul Kalam Centre for Innovation, University of Lucknow and Prof. Poonam Tandon, Department of Physics, University of Lucknow, Lucknow for providing the Gaussian software for optimized molecular structure. We also acknowledge Prof. Shailja Mahamuni, Pune University for providing $Cd_{1-x}Zn_xS/ZnS$ core/shell QDs.

References

1. Chen, Y; Peng F; Yamaguchi, T; Song, X; Wu, S-T. High Performance Negative Dielectric Anisotropy Liquid Crystals for Display Applications. *Cryst.* **2013**, 3, 483-503.
2. Kirsch, P.; Heckmeier, M.; Tarumi, K. Design and synthesis of nematic liquid crystals with negative dielectric anisotropy. *Liq. Cryst.* **1999**, 26, 449–452.
3. Kirsch, P.; Reiffenrath, V.; Bremer, M. Nematic liquid crystals with negative dielectric anisotropy: Molecular design and synthesis. *Synlett*. **1999**, 1999, 389–396.
4. Hird, M.; Goodby, J.W.; Toyne, K.J. Nematic materials with negative dielectric anisotropy for display applications. *Proc. SPIE*. **2000**, 3955, 15–23.
5. Ge, Z.; Zhu, X.; Wu, T.X.; Wu, S.T. High transmittance in-plane switching liquid crystal displays. *J. Disp. Technol.* **2006**, 2, 114–120.
6. Chen, Y.; Luo, Z.; Peng, F.; Wu, S.T. Fringe-field switching with a negative dielectric anisotropy liquid crystal. *J. Disp. Technol.* **2013**, 9, 74–77.
7. Kahn, F.J. Electric-field-induced orientational deformation of nematic liquid-crystals: Tunable birefringence. *Appl. Phys. Lett.* **1972**, 20, 199–201.
8. Takeda, A.; Kataoka, S.; Sasaki, T.; Chida, H.; Tsuda, H.; Ohmuro, K.; Sasabayashi, T.; Koike, Y.; Okamoto, K. A super-high image quality multi-domain vertical alignment LCD by new rubbing-less technology. *SID Symp. Dig. Tech. Pap.* **1998**, 29, 1077–1080.
9. Yun, H.J.; Jo, M.H.; Jang, I.W.; Lee, S.H.; Ahn, S.H.; Hur, H.J. Achieving high light efficiency and fast response time in fringe field switching mode using a liquid crystal with negative dielectric anisotropy. *Liq. Cryst.* **2012**, 39, 1141–1148.
10. Basu, R.; Iannacchione, G. S. Evidence for directed self-assembly of quantum dots in a nematic liquid crystal, *Phys. Rev. E.* **2009**, 80, 010701.
11. Gupta, S.K.; Singh, D.P.; Manohar, R.; Kumar, S. Tuning phase retardation behaviour of nematic liquid crystal using quantum dots. *Curr. Appl. Phys.* **2016,** 16, 79.

12. Seidalilir, Z; Soheyli, E; Sabaeian, M; Sahraei, R. Enhanced electrochemical and electro-optical properties of nematic liquid crystal doped with Ni:ZnCdS/ZnS core/shell quantum dots. *J. of Molliq.* **2020**, 320, 114373.
13. Misra, A. K.; Tripathi, P. K.; Pandey, K. K.; Singh, B. P.; Manohar, R. Dielectric properties and activation energies of Cu: ZnO dispersed nematic mesogen N-(4- methoxybenzylidene)-4-butylaniline liquid crystal. *J. Dispers. Sci. Technol*. **2020**, 41, 1283–1290.
14. Singh, S. Impact of Dispersion of Nanoscale Particles on the Properties of Nematic Liquid Crystals. *Cryst.* **2019**, 9, 475.
15. Rastogi, A.; Manohar, R.; Effect of graphene oxide dispersion in nematic mesogen and their characterization results. *Appl. Phy. A.* **2019**, 125,192.
16. Rastogi ,A.; Pathak ,G.; Srivastava ,A.; Herman ,J.; Manohar, R. $Cd_{1-X}Zn_XS$/ZnS core/shell quantum dots in nematic liquid crystals to improve material parameter for better performance of liquid crystal based devices, *J. Molliq.* **2018**, 255, 93–101.
17. Pandey, S; Vimal, T; Singh, D. P.; Gupta, S. K.; Tripathi, P; Phadnis, C; Mahamuni, S; Srivastava, A; Manohar, R. $Cd_{1-x}Zn_xS$/ZnS core/shell quantum dot ferroelectric liquid crystal composite system: analysis of faster optical response and lower operating voltage. *Liq. Cryst.* **2014**, 41, 1811 – 1820.
18. Singh, D.P.; Pandey, S.; Gupta, S.K. ; Manohar, R.; Daoudi, A.; Sahraoui, A.H.; Phadnis, C.; Mahamuni, S. Quenching of photoluminescence and enhanced contrast of ferroelectric liquid crystal dispersed with $Cd_{1-X}Zn_XS$/ZnS nanocrystals. *J. Lumin.* **2016,** 173, 250.
19. Tripathi, P.K.; Joshi, B.; Singh, S. Pristine and quantum dots dispersed nematic liquid crystal. Impact of dispersion and applied voltage on dielectric and electro - optical properties. *Opt. Mater.* **2017**, 69, 61–66.
20. Petrescu, E.; Cirtoaje, C.; Danila, O. Dynamic behavior of nematic liquid crystal mixtures with quantum dots in electric fields. *Beilstein J. Nanotechnol.* **2018**, 9, 399–406.
21. Bae, W. K.; Nam, M. K.; Char, K.; Lee, S.; Gram-scale one-pot synthesis of highly luminescent blue emitting Cd_{1-x}ZnxS/ZnS nanocrystals. *Chem.Mater.* **2008**, 20, 5307–5313.
22. Bera, D.; Qian, L.; Kuan Tseng, T.; Holloway, P.H.; Quantum dots and their multimodal applications: a review, *Mater.* **2010**, 3, 2260–2345.

 doi:10.20944/preprints202103.0386.v1

23. Rastogi, A; Pandey, F. P.; Parmar, A. S.; Singh, S; Hegde, G; Manohar, R. Effect of carbonaceous oil palm leaf quantum dot dispersion in nematic liquid crystal on zeta potential, optical texture and dielectric properties. *J Nanostruct Chem.* **2021**.
24. Rastogi, A; Hegde, G; Manohar, T; Manohar, R. Effect of oil palm leaf – based carbon quantum dot on nematic liquid crystal and its electro – optical effects. *Liq. Cryst.* **2020**.